EPSC Abstracts
Vol. 12, EPSC2018-68, 2018
European Planetary Science Congress 2018

The Banded Terrain on the Hellas Basin Floor, Mars: Gravity-driven flow not Supported by New Observations

Hannes Bernhardt (1,2), Mikhail Ivanov (3), Dennis Reiss (1), Harald Hiesinger (1), Ernst Hauber (4), Jaclyn D. Clark (2) (1) Westfälische Wilhelms-Universität, Institut für Planetologie, Münster, Germany (2) Arizona State University, School of Earth and Space Exploration, Tempe, AZ, USA (3) Vernadsky Institute, Russian Academy of Sciences, Moscow, Russia (4) Institut für Planeten- forschung, Deutsches Zentrum für Luft- und Raumfahrt, Berlin, Germany (h.bernhardt@asu.edu)

Abstract

We performed comprehensive, statistical geomorphologic analyses of the banded terrain, a ~30,000 km² area on the northwestern Hellas basin floor characterized by a Dm- to km-scale pattern of curvilinear troughs. The texture pattern does neither conform to topography nor exhibits regional (> 10s of km-scale) arrangements. Due to its association with glaciofluvial landforms (potential eskers and sandur plains) we tentatively propose a formation of the banded terrain as viscous till that was deformed by glacial overburden pressure.

1. Introduction

The western Hellas basin floor on Mars (Fig. 1 inlet) hosts a complex landscape containing several unique land- forms in close geographic association, e.g., the "honey- comb" and "banded" (or "taffy pull") terrains [e.g., 1-4]. Recent investigations concluded the honeycomb terrain to be truncated diapirs, possibly of salt or ice [3,5]. However, while periglacial features have been observed on the enigmatic banded terrain [1,3,6], its nature, formation, and thus its implications for the geologic, as well as climatic history of the Hellas basin remain largely unknown.

2. Data and methods

In order to resolve the textures of the banded and honeycomb terrains over their entire ex- tents, we produced a 1:175,000 photogeologic map encompassing an area of ~159,700 km² between 50°E 33.4°S and 61.3°E 44.3°S on the west-northwestern Hellas basin floor. The mapping process was carried out on a purpose-built, seamless CTX [e.g., 7] mosaic alongside version 12 of the THEMIS-IR Day Global Mosaic [8] and the global MOLA DEM [9]. Local-scale observations, including multi-temporal investigations, were made using HiRISE [10] as well as MOC-NA [11] images. Based on the CTX mosaic and MOLA DTM, we also performed a grid mapping (2x2 km grid size) of the entire banded terrain to assess its relation to local slopes (Fig. 1).

3. Observations

The characteristics of the banded terrain have been described in detail by [1,3,4]. In our map it covers over 30,000 km² and is subdivided into two subtypes. The creviced type (light blue/grey) is a smooth surface dissected by curvilinear troughs ("inter-bands" [1]). The ridged type (navy blue) has a rougher surface and shows the same general texture, but produced by ridges with the same dimensions as the troughs. In some locations, ridged type areas appear to superpose creviced type areas. Individual bands appear to interact in both, brittle and duc- tile manners (e.g., HiRISE PSP_008269_1395 showing one band "breaking" through another, causing slab rotation). Comparisons of MOC-NA with HiRISE images taken up to 14 years apart show no discernible change within the banded terrain (e.g., collapse by de-volatilization). The banded terrain superposes the honeycomb terrain (e.g., partially filling several honeycomb cells) as well as the hummocky, more elevated interior formation of the Hellas basin. Along its transition to the lower "Hellas Planitia trough" in the northwestern basin, the material of the interior formation appears as elongate mesas embayed by banded terrain. In many locations, band orientations are aligned to the mesas, or terminate on one side and continue on the other. Several large crater ejecta (e.g., Beloha crater) superpose the banded terrain. In certain locations, e.g., at 57,66°E 35,67°S, ejecta appears to be dissected by bands of the underlying banded terrain (e.g., north of Kufstein crater). According to our grid mapping (Fig. 1) the orientation of bands does not seem to correlate with the local slope. All grid box categories (Fig. 1 inlets) are nearly equally abundant

and distributed randomly, except within the honeycomb cells (circular arrangements dominant) and in the northernmost extents (lobate/slope-perpendicular arrangements dominant). In general, the banded terrain occurs across an elevation spectrum of almost 2 km, from -7667 m up to -5548 m. Within this spectrum, the creviced type follows a quasi-Gaussian distribution, whereas the ridged type occurs mostly below ~ -7,000 m.

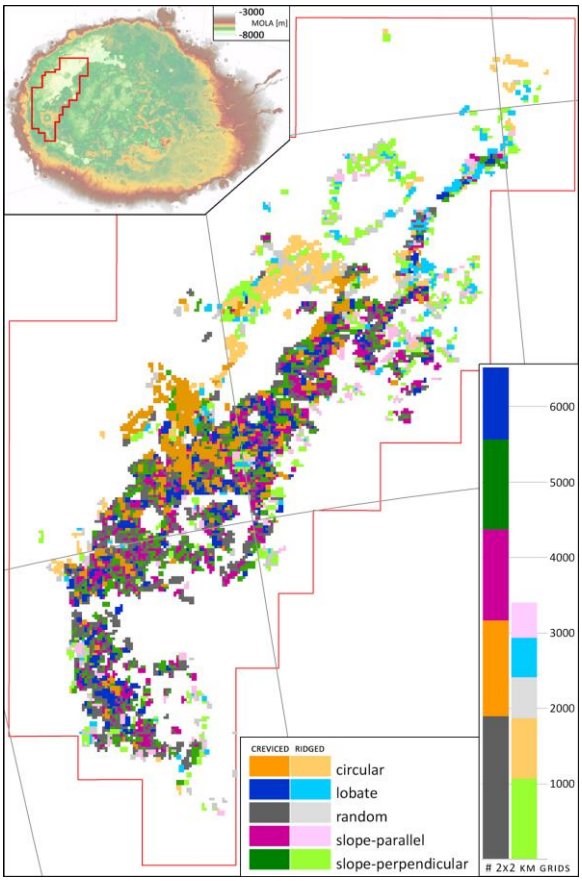

Figure 1: Grid mapping (2x2 km grid size) covering the entire banded terrain (light and navy blue units in (A)). The inlets show the different categories (defined by the banded terrain's relation to the local slope) assigned to grid boxes, as well as their respective abundances, i.e., number of grid boxes (cumulative bar chart). The inlet in the upper left shows the map's location on a color-coded MOLA view of the Hellas basin floor.

4. Discussion and conclusions

Based on previous [1,3,6,12] and new observations, it is highly unlikely that the banded terrain is the surface expression of a deeply rooted unit (e.g., truncated layers displaced by ductile de- formation during honeycomb formation [13-15]). Instead, the banded terrain seems to be a relatively thin, draping unit that experienced intense, mostly ductile, deformation at relatively shallow depths or at the surface. This viscous behavior, as well as the occurrence of periglacial landforms (e.g., thermokarst-like depressions) [1,3,6], imply a high volatile content in the past. However, its generally elevated thermal inertia (based on THEMIS), along with outcrops and small ejecta containing up to decameter-scale blocks [12], indicate that the banded terrain has since been compacted/cemented and desiccated, probably by katabatic winds. Such winds were suggested to be pervasive in this area [16,17] and likely cause ongoing deflation. Hence, we interpret the ridged type of the banded terrain as degraded version of the creviced type, with the ridges being clastic dikes of material that once filled the crevices. This is in agreement with the ridged type predominantly occurring in the lowest elevations of the unit's extent, where deflation is expected to be more intense [3,17]. Contrary to a previous assessment [1], our observations (band orientations not correlating with the local slopes of modern topography) do not support gravity-driven flow as the source of deformation that resulted in today's banded terrain. Instead, our investigation implies numerous, small- scale, slope-independent stress fields (<10s of km) of different orientations. These stress fields must have sufficed not only to deform the banded terrain, but also to deform superposing crater ejecta in certain locations (e.g., at 57,66°E 35,67°S). Furthermore, as no regional pattern (>10s of km) can be identified within the banded terrain, we suggest that large-scale, regional stress fields had little or no effect on its deformation. "Band hierarchies", i.e., bands overlapping or apparently breaking through each other, indicate multiple phases of deformation, possibly at different strain rates. One possible yet inconclusive formation model for the banded terrain might be a wet-based, subglacial environment, in which ductile material was deformed in stress fields caused by the ice overburden pressure. This pressure acted in conjunction with bed topography as well as zones of variable surging and basal decoupling, resulting in various different strain rates and band arrangements.

References: [1] Diot, X. et al. (2015) JGR: Planets, 120(12), 2258–2276. [2] Bernhardt et al., (2016) Icarus, 265, 407-442. [3] Bernhardt et al., (2016) JGR: Planets, 121, 714-738. [4] Voelker at al. (2017) PSS, 145, 49-70. [5] Weiss and Head (2017) Icarus, 284, 249-263. [6] Diot et al. (2014) PSS, 101, 118-134. [7] Malin, M. C. et al. (2007) JGR, 112(E5), E05S04. [8] Edwards et al. (2011) JGR: Planets, 116, E10008 . [9] Smith, M. D. et al. (2001) JGR, 106(E10), 23689. [10] McEwen, A. S. (2007) JGR, 112, E05S02. [11] Malin, M. C., & Edgett, K. S. (2010) The Mars Journal, 5, 1–60. [12] Diot, X. (2015) PSS, 121, 36–52. [13] Moore and Wilhelms (2001) Icarus 154, 258-276. [14] Mangold and Allemand (2003) Int. Conf. Mars#3047. [15] Kite et al., (2009) LPSC#1249. [16] Siili, T. (1999) PSS, 47(8–9), 951–970. [17] Howard et al. (2012) LPSC#1105.